



## Structural modifications and augmented affinity for bile salts in enzymatically denatured egg white

Chunjie Liu<sup>a</sup>, Yating Wu<sup>a,1</sup>, Guoguo Jin<sup>a</sup>, Baocai Xu<sup>a</sup>, Lin Mei<sup>a,b,\*</sup>

<sup>a</sup> College of Tea and Food Science, Anhui Agricultural University, 130 Changjiang West Road, Hefei, 230036, Anhui, PR China

<sup>b</sup> Key Laboratory of Agricultural Product Fine Processing and Resource Utilization, Ministry of Agriculture and Rural Affairs, 130 Changjiang West Road, Hefei, 230036, Anhui, PR China

### ARTICLE INFO

#### Keywords:

Egg white protein  
Bile salts binding ability  
*In vitro* simulation of gastrointestinal digestion  
Structure-activity relationship

### ABSTRACT

Protein binding to bile salts (BSs) reduces cholesterol levels, but the exact mechanism is unclear. In this study, we performed simulated gastrointestinal digestion of egg white protein hydrolysate (EWP) and included an unenzyme digestion group (CK) to investigate the changes in BSs binding capacity before and after digestion, as well as the relationship between egg white protein (EWP) structure and BSs binding capacity. In addition, peptidomics and molecular docking were used to clarify EWP's binding mechanism. We found that the BSs binding ability of EWPHs was slightly decreased after digestion, but significantly higher than that of the CK group and the digested CK group (D-CK). Particle size analysis and electrophoresis demonstrated that smaller particles and lower molecular weights exhibited enhanced binding capacity to BSs. Fourier Transform infrared spectroscopy (FTIR) results revealed that a disordered structure favored BS binding ability enhancement. Peptides FVLPM and GGGVW displayed hypocholesterolemic efficacy.

### 1. Introduction

Cardiovascular disease is the leading cause of human mortality, and high cholesterol is one of its risk factors. Currently, statins have demonstrated significant effectiveness as cholesterol-lowering agents (Besseling, Kastelein, & A, 2016). However, these medications also pose potential safety concerns, primarily due to their possible side effects, including abnormal blood sugar levels, muscle weakness and myalgia, liver enzyme abnormalities, as well as impairments in memory and cognitive function. Therefore, prevention and cholesterol lowering through dietary modifications are of great importance. Among them, bile salts-binding (BSs-binding) is one of the ways to lower cholesterol. The BSs-binding ability of proteins has been reported, but the mechanism of both binding is not clear.

BSs are sodium or potassium salts formed by the combination of bile acids secreted by hepatocytes with glycine or taurine. When BSs are excreted into the small intestine with liver bile, about 95% of them are absorbed into the blood at the end of the ileum, and then enter the liver through the portal vein to synthesize bile again and then excreted into the intestine. This process is part of the intestinal-hepatic circulation (Alberto, Ignasi, Sofia, Jaume, & Enric, 2023). Since cholesterol is

degraded into bile acids in the body, it plays a vital role in regulating cholesterol metabolism and is an important factor in preventing heart attacks and other cardiovascular diseases. Therefore, inhibition of bile acid reabsorption allows for cholesterol degradation in the liver, thus reducing blood cholesterol levels (Bellesi & Pilosof, 2021). The most abundant BSs in the human body are taurocholate, glycocholate, and deoxycholate. These particular types of surfactants have unusual properties closely related to their biological functions. A bile acid binding protein known as MRJP1 (major RJ protein 1) was isolated from royal jelly, which is a cholesterol-lowering food, and the isolated protein binds taurocholate *in vitro* and reduces cholesterol uptake by Caco-2 enterocytes (Kashima et al., 2014). Chen et al. (2020) found that the hydrolysate obtained by fermentation of celery seed protein with *Bacillus subtilis* showed strong bile salt binding ability *in vitro*, and the molecular weight range was 7.8–11.5 kDa. However, although these studies illustrated the cholesterol-lowering function of the protein bound to BSs, they did not delve into the mechanism of action of its binding.

Egg whites are the main component of eggs, consisting of 88% water and 12% solids, of which >90% is protein and the rest is a very small amount of lipids, vitamins and minerals. There are >40 types of proteins in egg whites, containing 8 essential amino acids, with a human

\* Corresponding author at: College of Tea and Food Science, Anhui Agricultural University, 130 Changjiang West Road, Hefei 230036, Anhui, PR China  
E-mail address: [meilin8880@sina.com](mailto:meilin8880@sina.com) (L. Mei).

<sup>1</sup> Co-first author

<https://doi.org/10.1016/j.fochx.2024.101577>

Received 30 April 2024; Received in revised form 6 June 2024; Accepted 17 June 2024

Available online 22 June 2024

2590-1575/© 2024 Published by Elsevier Ltd. This is an open access article under the CC BY-NC-ND license (<http://creativecommons.org/licenses/by-nc-nd/4.0/>).

digestibility and absorption rate of >98%, making them one of the most desirable protein resources in food (Abeyrathne, Huang, & Ahn, 2018). Ovalbumin (OVA), ovotransferrin (OVT), and ovomucoid are the major proteins, while lysozyme, ovalbumin, oval mucin, and yolk protein are the minor proteins in egg whites. Therefore, egg white protein (EWP) is considered to be a very valuable protein resource and has better excellent functions such as foaming, emulsification and gelling. Currently, a small number of studies have found that EWP has the ability to lower cholesterol (Abeyrathne et al., 2018). However, studies investigating the cholesterol-lowering efficacy and binding mechanism of EWP through the BSs binding pathway have not been reported.

Therefore, in this study, the EWP was used as a raw material, modified by enzymatic digestion technique. And the effect of digestion on the structural and functional properties of EWP was explored based on *in vitro* simulated gastrointestinal digestion. Furthermore, peptidomics were used to find the target functional peptides, and the binding mechanism was clarified by prediction and molecular docking between egg white protein and BSs molecules.

## 2. Materials and methods

### 2.1. Materials

EWP were obtained from special grade grass eggs (purchased from RTF, Hefei, Anhui Province), neutral protease (S10013, 100 U/mg), artificial gastric fluid (Chp), artificial small intestine fluid (containing pancreatic enzymes and phosphate) and sodium taurocholate (STC) were purchased from Yuanye Biological Co., Ltd. (Shanghai, China). Sodium cholate (SC) and sodium deoxycholate (SDC) were purchased from Macklin Biochemical Technology Co., Ltd. (Shanghai, China).

### 2.2. Preparation of the EWPHs

EWP solution with a substrate concentration of 8% (v/v) was prepared and pH 7.0 was maintained using 0.5 M HCl and 0.5 M NaOH. Neutral protease was used and enzymatic digestion was performed at an enzyme specific activity of 6000 U/g (enzyme/EWP), enzymatic digestion time of 6 h, enzymatic digestion temperature of 37 °C and pH 7.0. The enzyme was subsequently inactivated at high temperature (90 °C, 10 min), cooled in an ice bath and then centrifuged at 10000 r/min for 10 min at 4 °C. The supernatant was freeze-dried and stored in a refrigerator at 4 °C for the determination of BSs-binding rate.

### 2.3. *In vitro* simulation of gastrointestinal digestion

Referring to the method of Yang et al. (2021) with slight modifications, 80 mg/mL of EWP solution was prepared, and the pH was adjusted to 2.0 with 1 M of HCl solution. EWP solution (10 mL) was mixed with gastric digestion (20 mL) solution (containing pepsin, 2000 U/mL), and the mixed solution was shaken continuously (110 r/min) at 37 °C to simulate gastric digestion for 60 min. Immediately after the gastric digestion phase, the pH was adjusted to 7.0 with 1 M NaOH, and 30 mL of the gastric digestion mixture was mixed with an equal volume of artificial small intestine solution (containing pancreatic enzyme, 2000 U/mL), and the mixture was shaken continuously (110 r/min) at 37 °C for 120 min to simulate intestinal digestion. Then, the reaction was terminated at high temperature and cooled in an ice bath for 30 min to stop the digestion process. At the end of the reaction, the digest was centrifuged at 4 °C and 4500 r/min for 15 min. The supernatant was freeze-dried and stored at -20 °C for subsequent determination of the BSs binding rate.

### 2.4. BSs-binding capacity

#### 2.4.1. Standard curve of BSs

The standard curve was prepared according to the method with

slight modifications (Milkiewicz, Roma, Elias, & Coleman, 2002). STC, SC and SDC solutions (0.4 mM) were prepared using phosphate buffer solution (0.1 M, pH 6.3, phosphate buffer solution, PBS). Into separate centrifuge tubes, 0, 0.5, 1.0, 1.5, 2.0, 2.5 mL of STC, SC, or SDC solutions were added, followed by the addition of 2.5 mL of sample solution and 7.5 mL of sulfuric acid solution (H<sub>2</sub>SO<sub>4</sub>, 60%, v/v). After cooling the samples rapidly with ice water, the enzyme marker was used to determine the absorbance value at 387 nm. Each BS was plotted as a horizontal coordinate and a vertical coordinate based on its concentration. Each group of samples was subjected to three parallel tests.

#### 2.4.2. Determination of BSs binding capacity

Referring to the method of Yoshie-Stark and Waesche (2004), 1 mL (60 mg/mL) of EWP samples and 4 mL of BSs solution (0.4 mM STC, SC, and SDC, prepared with PBS solution) were taken, shaken in an incubator at 37 °C for 2 h, and then centrifuged in a centrifuge (4000 r/min, 20 min). Supernatant (2.5 mL) is mixed with 7.5 mL of H<sub>2</sub>SO<sub>4</sub> solution (60%, v/v), soaked for 20 min at 70 °C, removed and cooled immediately with ice water. A 387 nm absorbance value can be determined using an enzyme marker, and a standard curve can be used to calculate the concentration of BSs in the solution. As a control, 1 mL of PBS buffer solution was used instead of the sample [Eq.1]:

$$BS(\%) = \frac{C_0 - C_1}{C_0} \times 100 \quad (1)$$

where C<sub>0</sub> is the BSs concentration of the control solution, mM; C<sub>1</sub> is the BSs concentration in the supernatant of EWP, mM.

### 2.5. Determination of total sulfhydryl groups

For the determination of total sulfhydryl groups refer to the method of Shen, Fang, Gao, and Guo (2017). Following the methodology described by Shen et al. (2017), EWP samples were diluted to a concentration of 5 mg/mL. Subsequently, 0.2 mL of the diluted sample was added to a centrifuge tube along with 1 mL of buffer solution 3 and 0.02 mL of mercaptoethanol. The solution was then thoroughly mixed. The reaction was carried out at 25 °C for 1 h, then 10 mL of 12% TCA was added and centrifuged at 5000 rpm for 15 min. The supernatant was removed and suspended in 5 mL 12% TCA, centrifuged for 10 min, and then centrifuged twice. After the supernatant was removed, 3 mL buffer solution 2 and 0.03 mL Ellman reagent were added. The calculation formula is as follows [Eq.2]:

$$-SH \left( \mu\text{mol/g prot} \right) = \frac{(73.53 \times A_{412} \times D)}{C} \quad (2)$$

where A<sub>412</sub> is the absorbance value at 412 nm; D is the dilution of EWP samples; D = 15.15; C is the protein concentration, mg/mL.

### 2.6. Sodium dodecyl sulphate-polyacrylamide gel electrophoresis (SDS-PAGE) and Tricine-SDS-PAGE analysis

Based on the method described by Li et al. (2021), the preparation of 12% isolate and 5% concentrate gels were conducted. Subsequently, the molecular weight distribution of the samples was analyzed using SDS-PAGE. For this analysis, a Tricine-SDS-PAGE system with 16.5% separation gel, 10% interlayer gel, and 4% concentration gel was employed. The specific experimental process can be found in the appendix.

### 2.7. UV absorption spectroscopy

The protein samples were diluted to 0.1 mg/mL with PBS solution (0.01 mol/mL, pH 7.0), and distilled water was used as a blank, and the UV spectra were scanned at a scan rate of 100 nm/min in the range of 200–600 nm (Pi et al., 2021).

## 2.8. Intrinsic fluorescence spectrum

According to the method of Xu, Xia, and Jiang (2012) with slight modifications, protein samples were diluted to 0.1 mg/mL with PBS solution (0.01 mol/mL, pH 7.0), distilled water was used as a blank, and endogenous fluorescence spectra were measured by fluorescence spectrophotometer. The excitation wavelength is 295 nm, the width of excitation and emission slit is 5 nm, the scanning speed is 1200 nm/min, and the scanning range is 300–450 nm.

## 2.9. Surface hydrophobicity ( $H_0$ )

The surface hydrophobicity ( $H_0$ ) of the samples was determined according to the method of Pessato et al. (2016) with slight modifications. A solution of ANS at a concentration of 8 mM was obtained using 1-phenyl naphthalene-8-sulfonic acid (ANS) as an anionic fluorescent probe dissolved in 0.01 M, pH 7.0, sodium phosphate buffer. The samples were diluted in 0.01 M sodium phosphate buffer (pH 7.0) in the range of 0.05–0.25 mg/mL. 10  $\mu$ L of ANS solution was mixed with 2 mL of sample diluent and reacted in a dark environment for 15 min. Then the fluorescence intensity of the obtained solution was monitored by a fluorescence spectrophotometer. The excitation wavelength is 390 nm and the scanning emission spectrum is 400–750 nm. A linear regression was used to fit a plot of fluorescence intensity (the highest fluorescence intensity at the same emission wavelength for different concentrations) versus protein concentration, and  $H_0$  for EWP samples was expressed as the slope of the curve.

## 2.10. FTIR

Changes in EWP functional groups in different treatment groups were investigated by FTIR of lyophilized samples according to the method of Li et al. (2021) and changes in secondary structure were estimated after cross-linking. In order to prepare the spectra, a mixture of 100 mg of potassium bromide (KBr) and 1 mg of sample was ground and sliced into thin slices. With a resolution of 4  $\text{cm}^{-1}$ , the scanning wave number was between 4000  $\text{cm}^{-1}$  and 400  $\text{cm}^{-1}$ . These bands are attributed to the secondary structure of the protein in the amide I region (1600–1700  $\text{cm}^{-1}$ ). The amide I band in the spectrum was analyzed by OMSNIC and Peakfit software. In order to visualize the secondary structure components of proteins, we created stacked plots using Origin software.

## 2.11. Rheological properties

Referring to the method of Gu, Campbell, and Euston (2009), the EWP sample solution (100 mg/mL) was slowly poured onto a 40 mm diameter plate fixture. The apparent viscosity and shear stress of the WPI samples were measured using a rheometer at a shear rate of 0.1–300  $\text{s}^{-1}$ . A 500 mL of LEWP solution was prepared. The dynamic rheological properties of different WPI solutions were determined using a 40 mm diameter plate with a spacing of 1 mm. This plate had a measurement temperature of 20  $^{\circ}\text{C}$ , a strain of 10%, and an angular frequency of 0.1–100 rad/s. Under these conditions, different EWP solutions exhibit different dynamic rheological properties.

## 2.12. Scanning electron microscopy (SEM)

The experiment was conducted using a scanning electron microscope (SU1510, Hitachi, Japan). Images were observed at a gold spray current of 15 mA, at an accelerating voltage of 15.0 kV, at a working distance of 9.4 mm, at a working temperature of 25  $^{\circ}\text{C}$ , and at a magnification of  $150\times$ .

## 2.13. Measurement of particle size

Using laser particle size analyzer, the particle size of each sample was determined according to Hu, Li-Chan, Wan, Tian, and Pan (2013): 5% (w/v) protein solution was prepared by dispersing the sample in distilled water, using water as dispersant, the refractive index of particles was 1.45, 1.33 and 0.001 respectively. The average particle size is expressed by volume average diameter D [4, 3].

## 2.14. Peptidomics analysis

The peptidomic analysis was based on high-performance liquid chromatography-tandem mass spectrometry (LC-MS/MS). The specific experimental process can be found in the appendix.

## 2.15. Molecular docking

Docking simulations of proteins in egg white interacting with BSs molecules were performed using AutoDock software and modified to follow the method of Wang et al. (2022). To predict the interaction forces between ovalbumin and BSs molecules, the PLIP website was used (<https://plip-tool.biotec.tu-dresden.de/plip-web/plip/index>). Furthermore, PubChem (<https://pubchem.ncbi.nlm.nih.gov>) contains 3D structures of ovalbumin (<https://doi.org/10.2210/pdb1JTI/pdb>). PubChem was used to obtain three-dimensional structures of sodium cholate, sodium taurocholate, and sodium deoxycholate. To reveal the interactions between ligands and receptors, default docking parameters are applied, a docking simulation is run with AutoDockTools, and selected docking results with the lowest docking energy are drawn using PyMol software.

## 2.16. Statistical analysis

The data were statistically processed by Excel (Microsoft 2019) and analyzed by SPSS software (IBM SPSS Statistics 22). LSD multiple comparison method was used for analysis of variance. Results were expressed as mean  $\pm$  standard deviation, with  $p < 0.05$  as the significance criterion. Plots were made using Origin 2019. All experiments were repeated three times.

## 3. Results and discussion

### 3.1. BSs binding capacity of EWP before and after digestion

The BSs binding capacities of the CK and EWPHs groups after *in vitro* simulated gastrointestinal digestion were shown in Fig. 1 (A). EWPHs were significantly higher than that of CK ( $p < 0.05$ ). There was a certain tendency for the BSs binding rate of the CK group to increase following digestion, while the BSs binding rate of the EWPH group decreased to some extent following digestion. However, the BSs binding rate of digested EWPHs (D-EWPHs) in both groups after digestion was still significantly higher than that of the D-CK group ( $p < 0.05$ ). Barbana, Boucher, and Boye (2011) found that lentil proteins subjected to *in vitro* simulated gastrointestinal digestion had significantly lower BSs binding capacities than undigested samples, suggesting that hydrophobic interactions may be responsible for this difference.

### 3.2. Total sulfhydryl groups

Sulfhydryl changes affect the structure and function of proteins, reflecting the formation and breaking of intramolecular and intermolecular disulfide bonds (Ai, Xiao, & Jiang, 2020). As shown in Fig. 1 (B), both enzymatic treatment and simulated gastrointestinal digestion resulted in a significant decrease in sulfhydryl content ( $p < 0.05$ ). As compared to CK, the sulfhydryl content of the enzymatically treated EWP was significantly lower in the EWPH group. In this case, its

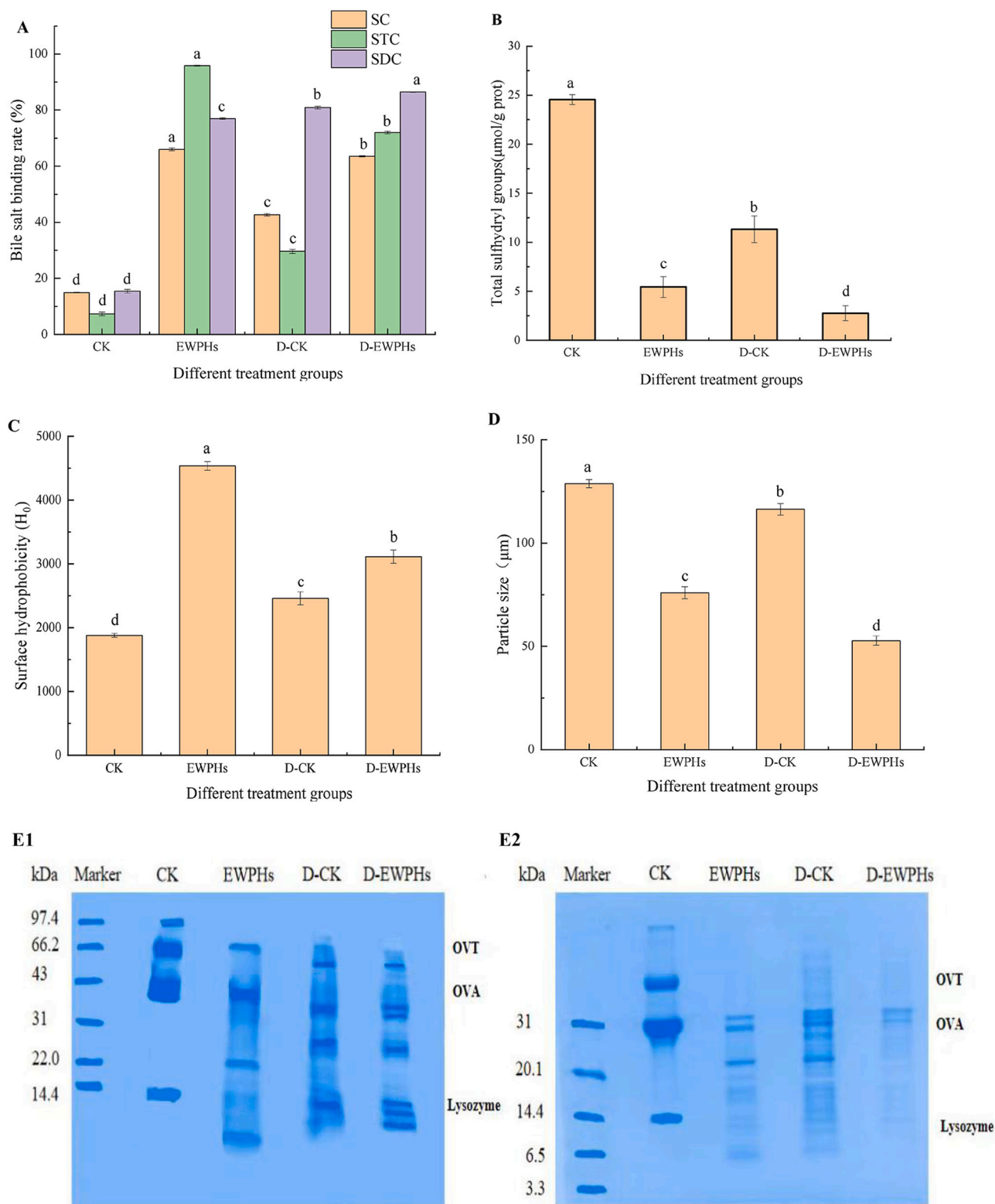


**Fig. 1.** (A) Bile salt binding rate of EWP in simulated gastrointestinal digestion before and after enzymolysis. Means with different lowercase (apply to comparisons among different bile salt at a distinct treatment) superscripts differ significantly ( $p < 0.05$ ), (B) Total sulphydryl content of CK, EWPHs, D-CK and D-EWPHs, (C) Surface hydrophobicity of CK, EWPHs, D-CK and D-EWPHs, (D) Particle sizes of CK, EWPHs, D-CK and D-EWPHs, and (E) SDS-PAGE (E1) and Tricine-SDS-PAGE (E2) of CK, EWPHs, D-CK and D-EWPHs.

conversion into disulfide bonds resulted in more disulfide bonds being formed. As a result of simulated gastrointestinal digestion, the sulfhydryl contents of both CK and EWPHs decreased. This was due to the further hydrolysis of proteins by pepsin and trypsin in the digestive fluid. This resulted in some hydrophobic groups being exposed, protein

aggregation, and sulfhydryl groups constantly being converted into disulfide bonds. Additionally, D-EWPHs contained significantly fewer sulfhydryl groups than D-CKs. As a result of simulated gastrointestinal digestion, enzymatically treated EWPs displayed significantly higher levels of protein defolding than untreated EWPs, resulting in a greater

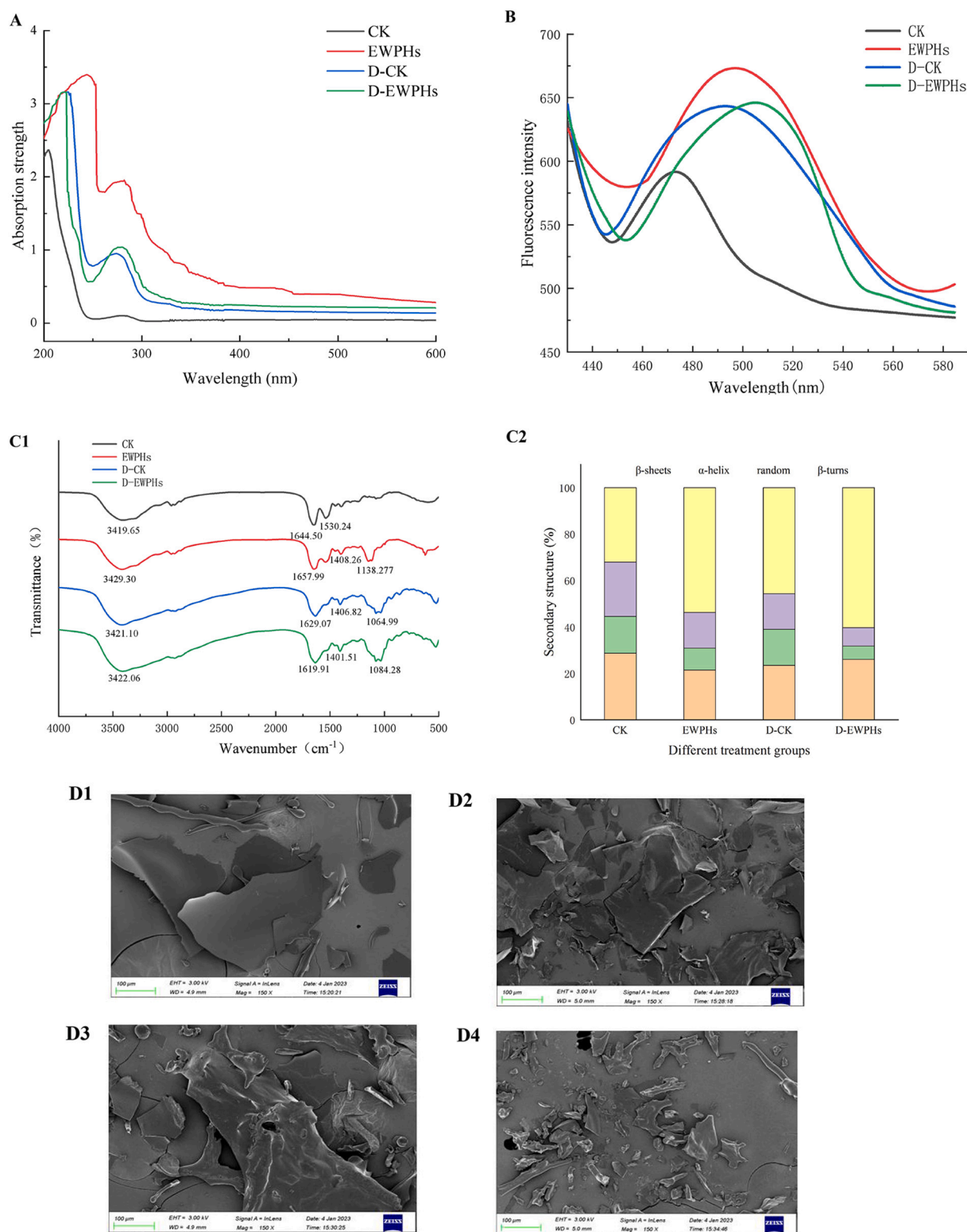


**Fig. 2.** (A) UV spectra of CK, EWPHs, D-CK and D-EWPHs, (B) Intrinsic fluorescence spectra of CK, EWPHs, D-CK and D-EWPHs, (C) FTIR spectra (C1) and secondary structure-occupied stacking maps (C2) of CK, EWPHs, D-CK and D-EWPHs, and (D) SEM images of EWP under different treatments (D1) CK group (D2) EWPHs group (D3) D-CK group (D4) D-EWPHs group.

amount of hydrophobic groups being exposed to the environment. In consequence, EWPHs were more able to bind to BSs due to the disulfide bond. This culminated in a cholesterol reduction.

### 3.3. UV absorption spectroscopy

As shown in Fig. 2 (A), the maximum UV absorption wavelength of EWP experienced varying degrees of blue or red shift before and after digestion by enzymes and simulated digestion by gastrointestinal tract. This was due to the combined effect of tyrosine, tryptophan and phenylalanine residues (Huang, Ding, Dai, & Ma, 2017). Compared with the CK group, EWPH UV absorption intensity increased and a certain amount of redshift occurred. It is probable that this is a result of the enzymatic digestion of EWP promoting its degradation and affecting its exposure to tyrosine and tryptophan residues. Pi et al. (2021) found that peanut proteins were autoclaved and fermented by *Bacillus subtilis*, resulting in an increase in UV absorption intensity and a red shift of 1–5 nm at 210 nm. This suggests that peanut proteins have been partially degraded and that peptide bonds hidden in protein aggregates are increasingly exposed, which confirms the hypothesis that they cause peanut proteins to unfold and tryptophan and tyrosine residues to be exposed. Upon simulated gastrointestinal digestion, D-CK showed an increasing trend compared to the CK group in terms of maximum absorption intensity. This was as a result of the altered structure of EWP protein caused by the combination of pepsin and trypsin actions, resulting in the exposure of additional peptide bonds hidden in protein aggregates. Although a slight decrease in maximum absorption intensity was observed compared to the pre-digestion group, it remained higher than in the post-digestion CK.

### 3.4. Intrinsic fluorescence spectrum

The endogenous fluorescence of proteins arises from the leap between different electronic energy levels of aromatic amino acids (tyrosine, tryptophan, and phenylalanine), and the fluorescence intensity is determined by the energy difference between these different levels. Additionally, the polarity of the microenvironment in which the amino acids are located influences their excited and ground state energies (Viseu, Carvalho, & Costa, 2004). Consequently, the endogenous fluorescence of proteins can provide a reliable indicator of changes in their tertiary structure.

Fig. 2(B) shows endogenous fluorescence spectra of EWP after simulated gastrointestinal digestion before and after enzymatic digestion. Compared with the CK group, the fluorescence intensity of both enzymatic digestion and digestion-treated samples was significantly enhanced. After enzymatic digestion of EWP, its maximum fluorescence emission wavelength was red-shifted and its maximum fluorescence intensity was significantly increased. This indicates that enzymatic digestion unfolded the internal structure of the protein molecule and exposed the tryptophan residues. Consequently, some hydrophobic groups were exposed, resulting in a greater intensity of fluorescence for EWP. When simulated gastrointestinal digestion was simulated *in vitro*, the maximum fluorescence emission wavelength was redshifted and the fluorescence intensity increased in the CK group. As a result of the digestion process, which involved the action of digestive enzymes, the protein structure and amino acid sequence were altered, which improved the exposure of tryptophan residues to polar environments (Nandy, Chakraborty, Nandi, Bhattacharyya, and Mukherjee, 2019). After digestion, EWPHs lost fluorescence intensity, but their maximum emission wavelength shifted toward a longer wavelength. Therefore, EWPHs are still capable of maintaining high fluorescence intensity after digestion. (For interpretation of the references to color in this figure legend, the reader is referred to the web version of this article.)

### 3.5. Surface hydrophobicity ( $H_0$ )

Surface hydrophobicity ( $H_0$ ) of a protein is a measure of the change in the hydrophobic group on the surface of the protein upon contact with the aqueous environment (Celus, Brijis, & Delcours, 2007). The degree of interaction between hydrophobic groups and the protein surface is usually reflected by changes in hydrophobic groups. Additionally, they reflect changes in the conformation and stability of proteins.

As shown in Fig. 1 (C), the  $H_0$  of EWPHs was significantly higher ( $p < 0.05$ ) compared to the CK group. This may be due to the fact that enzymatic treatment of EWP unfolded its internal structure and exposed hydrophobic residues, which in turn triggered a change in the distribution of hydrophobic regions of the protein (Li, Yang, Zhang, Ma, & Mahunu, 2016). According to Wang et al. (2023), proper enzyme digestion of EWP facilitated the appearance of hydrophobic sites, which led to a significant increase in  $H_0$ . Despite this,  $H_0$  exhibited a decreasing trend as enzyme addition increased. The aggregation of the protein may result in exposed hydrophobic groups hiding within the protein. Similarly, the surface hydrophobicity of EWPHs decreased after digestion in the present study. The reason for this is excessive enzymatic digestion that causes protein to aggregate and hide some hydrophobic groups. Conversely, the CK group was digested by digestive enzymes and pH, which resulted in protein deformation and unfolding, promoting protein de-folding, and exposing more hydrophobic groups, leading to an increase in  $H_0$ .

### 3.6. FTIR

As shown in Fig. 2 (C), the percentages of helices and sheets of EWPHs in the enzymatic digestion group decreased by 8.07% and 7.34%, respectively, compared to the control group. In contrast, the percentages of turns and disordered curls increased by 15.41%. In this respect, it should be noted that enzymatic digestion contributes to the transition from ordered to disordered structures. Wang et al. (2023) found a significant reduction in the proportion of  $\alpha$ -helix in EWP after enzymatic digestion. Ashraf, Liu, Awais, Xiao, and Zhou (2020) previously reported that after sonication, pro-sheets to irregular curls were converted in mung bean proteins, indicating that the sonication can disrupt cross-linkage bonds and alter amino acid sequences, thus affecting the function of hydrolysates, *i.e.* reducing cholesterol production. Liu et al. (2022) examined the secondary structure of soy protein and found that the ordered structure was converted into a disordered structure when enzymatic digestion, screw speed and heat were applied. It is believed that this phenomenon is the result of denaturation of the proteins and increased protein cross-linking under these conditions. After digestion of the CK group, the ratio of helix-to-sheet was reduced due to the digestive enzymes and a decrease in digestion fluid pH, which resulted in the enzymatic degradation of EWP, which in turn resulted in the unfolding of certain structures. Comparatively, the observed changes in the ordered and disordered structures of the EWPHs group were not statistically significant. According to Wang et al. (2023), no significant changes in EWP secondary structure occurred when enzymes were added to the mixture. The presence of digestive enzymes in the digestion solution does not significantly affect the secondary structure of enzymatically processed EWP. Thus, enzymatic digestion of EWP causes degradation of the protein and unfolding of the internal molecular structure, resulting in changes in its secondary structure with an increase in  $\beta$ -turns angle and some reduction in  $\alpha$ -helix,  $\beta$ -sheets and irregular coiling, as well as affecting the BSs binding capacity of EWP, indicating the effect of secondary structure on the cholesterol-lowering function of EWP.

### 3.7. SDS-PAGE, and Tricine-SDS-PAGE analysis

#### 3.7.1. SDS-page

As shown in Fig. 1 (E) after enzymatic treatment, compared to the

control group, egg transferrin and ovalbumin protein bands were significantly thinner, and the protein bands of lysozyme disappeared and new bands appeared in the part with a molecular weight <14 kDa, indicating that enzymatic digestion resulted in the degradation of EWP to produce small molecular peptides. It was found that after heating egg white powder and enzymatic treatment, all bands near 75 kDa disappeared and new bands appeared below ovalbumin located near 45 kDa, which was consistent with the results reported in this paper. According to Wang et al. (2023), enzymatic digestion promotes the degradation of protein macromolecules and produces peptides of functional small molecules. After simulated gastrointestinal digestion it was observed that new bands appeared near 22–43 kDa for D-CK, and new bands appeared below the bands of oval transferrin, ovalbumin and lysozyme for D-EWPHs, due to further degradation of proteins by digestive enzymes to generate more small molecules.

### 3.7.2. Tricine-SDS-PAGE

Since enzymatic digestion and simulated gastrointestinal digestion generated some small molecule polypeptides from EWP, small molecule gel electrophoresis was performed using SDS-PAGE. As shown in Fig. 1 (E2), the EWPH bands were mainly distributed between 6.5 and 31 kDa compared with the CK group. Therefore, it can be concluded that the large-molecule proteins in EWP have been degraded and the small-molecule bands have been aggregated under neutral proteases to produce more small-molecule polypeptides. In the D-CK (lane 4) group, after the digestive process was simulated, the bands became thinner, darker, and more numerous. Accordingly, EWP was enzymatically degraded after digestion by trypsin and pepsin to produce small molecule peptides. It is possible that this may be attributed to the increased ability to bind BSs. The binding capacity of pea hydrolysates obtained by alkaline protease enzymatic digestion was found to be between 7.8 and 11.5 kDa at the molecular weight of Klost, Giménez-Ribes, and Drusch (2020). It can be concluded that the peptides produced after enzymatic digestion of EWP may affect its ability to bind BSs.

### 3.8. Microstructure

In order to investigate the changes of microstructure of EWP before and after enzymatic treatment and simulated gastrointestinal digestion treatment, SEM was used for observation and analysis. From Fig. 2 (D1), it can be seen that the surface structure of the unenzymatic CK group was smooth and the proteins were in the shape of lamellar structures, while Fig. 2 (D2) shows the EWPHs obtained after enzymatic treatment. After the enzymatic treatment of EWP, the lamellar structure of the protein surface was destroyed and showed irregular small fragment shapes with a looser structure. This is because enzymatic digestion destroys the internal structure of the protein and forms proteins or peptides with smaller molecular weights. Fig. 2 (D3) shows the D-CK group, after digestion, the protein surface became rough and partially cleaved, which may be the result of the action of digestive enzymes. In contrast, the particle distribution in the D-EWPHs group (Fig. 2 (D4)) was more fragmented than that in the EWPHs group and there was protein aggregation. This phenomenon may be attributed to the unfolding of proteins after enzymatic and digestive treatment, which exposes excess hydrophobic groups and thus improves the BSs binding ability of EWPHs.

### 3.9. Particle size

As shown in Fig. 1 (D), enzymatically modified EWP had a different mean particle size before and after digestion. A significant difference was observed between the mean particle size of the EWPHs group and the CK group after enzymatic digestion. The reason for this was that the EWP generally aggregated with large proteins molecules and consisted of larger particles when it was not enzymatically digested. As a result of enzymatic digestion, these proteins were destroyed and degradation took place to produce small molecules. This is in accordance with the

results published by Xie et al. (2023) regarding rice protein hydrolysates. It was found that both groups of CK and EWPHs showed a reduction in mean particle size after simulated digestion in the gastrointestinal tract. It is possible that digestive enzymes are responsible for this. It was observed in the study by Colosimo, Mulet-Cabero, Warren, Edwards, and Wilde (2020) that intestinal digestion with trypsin resulted in an overall decrease in particle size when BSs were bound to fungal proteins. Overall, the average particle size of EWP kept decreasing as the BSs binding capacity increased, suggesting a relationship between particle size and BSs binding capacity, and the results shown in Fig. 1 (D) correspond to those of SEM, secondary structure, suggesting that enzymatic digestion disrupts the non-covalent fitness and electrostatic and hydrophobic interactions between EWP molecules, thus reducing the particle size of the protein and increasing the BSs binding capacity.

### 3.10. Rheological dynamics

#### 3.10.1. Static rheology

As shown in Fig. 3 (A), it was observed that the apparent viscosity of different treatment groups decreased with the increase of shear rate, indicating a thinned shear layer. According to Karaman, Yilmaz, Dogan, Yetim, and Kayacier (2011), this is a pseudoplastic fluid for non-Newtonian fluids. Among the other treatment groups, the CK group had the lowest level of viscosity. However, the viscosity of the enzymatically treated EWP was the highest. It was followed by D-EWPHs and D-CK. The apparent viscosity of the CK group increased at the same shear rate after enzymatic treatment, which may be due to the increased hydrophobic groups exposed to EWP due to the neutral protease activity. Consequently, protein molecules formed a three-dimensional mesh structure, which reduced mobility, resulting in tighter connections between protein molecules and increased apparent viscosity (Liu & Tang, 2014). In both the CK and EWPH groups, the apparent viscosity changed differently after digestion. As a consequence, D-CK's apparent viscosity increased while D-EWPH's viscosity decreased at the same shear rate. As a result of enzymatic activity and pH fluctuations during the process of digestion, this phenomenon may occur. Due to excessively acidic or alkaline pH levels, proteins undergo partial denaturation, leading to a weakened hydration layer on the surface of the protein solution. Consequently, intermolecular aggregation of proteins takes place, resulting in larger molecules that enhance the viscosity of the protein solution. In addition, it may be due to an increase in viscosity as the amount of homogeneous charge on the protein surface increases as it moves away from the isoelectric point (Malhotra & Coupland, 2004). As shown in Fig. 3 (B), with the increasing shear rate, the shear stresses all show an upward trend, in the following order: EWPHs > D-EWPHs > D-CK > CK. Where the shear stress of EWPHs is the highest, and the corresponding apparent viscosity is also the highest. Hence, apparent viscosity trends are correlated with shear stress.

#### 3.10.2. Dynamic rheology

Fig. 3 (C) and (D) shows the variation of energy storage modulus ( $G'$ ) and loss modulus ( $G''$ ) of EWPHs with the increase of angular frequency for different treatment groups, where the elastic properties are represented by  $G'$  and the viscosity is represented by  $G''$ . It can be seen from Fig. 1–5 that both  $G'$  and  $G''$  of the four groups of samples increase with angular frequency, in the following order: EWPHs > D-EWPHs > D-CK > CK. And  $G'$  is obviously larger than  $G''$ , which indicates that EWP's elastic property is larger than the viscous property. Compared with the CK group, the viscoelasticity of EWPHs increased, which indicates that enzymatic treatment of EWP can promote the formation of a homogeneous, compact and high-strength protein network gel structure (Liu, Xu, Zhao, & Yang, 2017). The CK group also showed a significant increase in viscoelasticity after digestion, which, in addition to the effect of digestive enzymes, may also be caused by changes in pH in the digestive environment. The pH changes cause denaturation of subunits in the protein and oxidation of sulfhydryl groups to generate disulfide

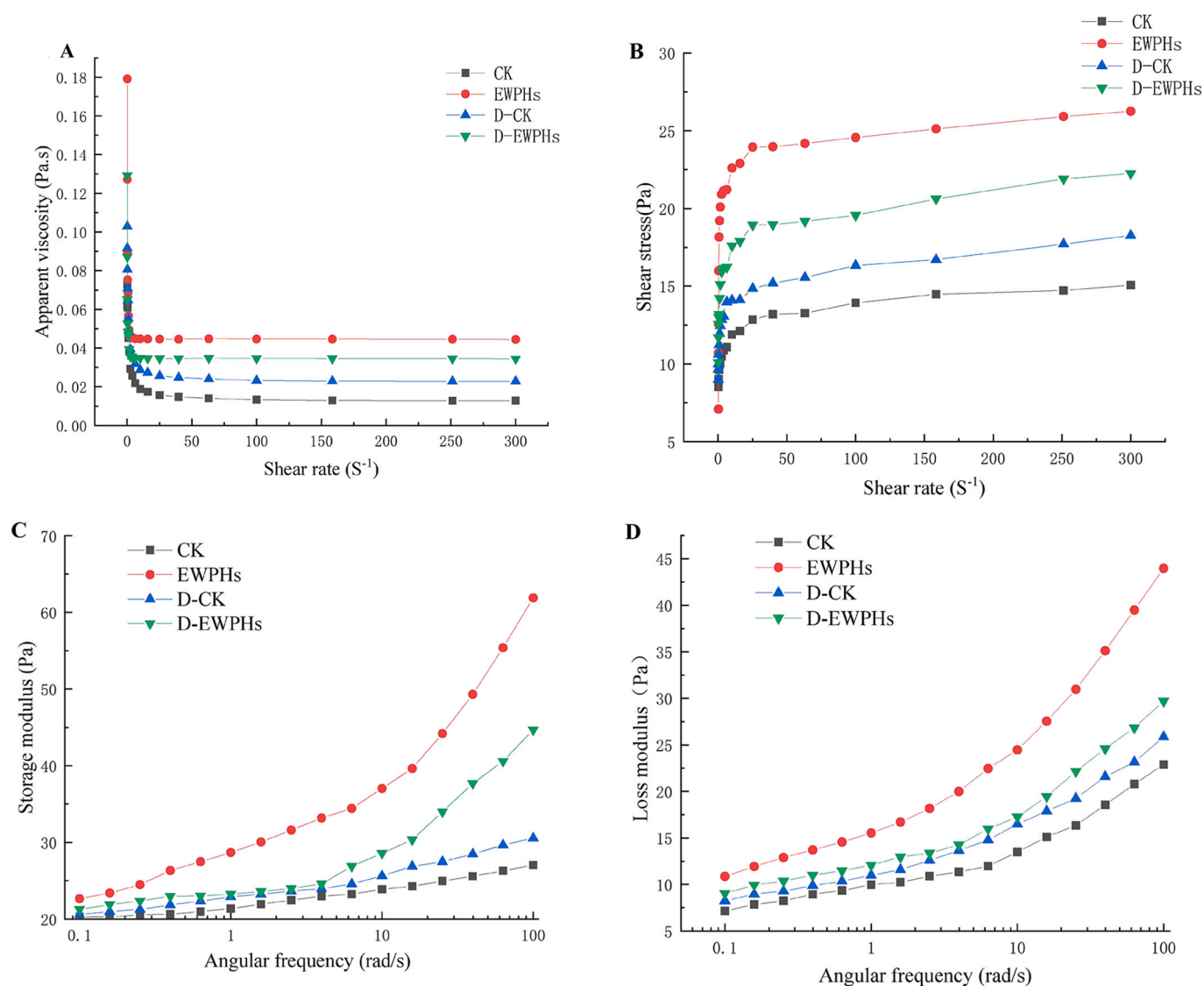


Fig. 3. Effect of different treatments on rheological properties of EWP: (A) Apparent viscosity, (B) Shear stress, (C) Storage modulus, and (D) Loss modulus.

bonds, and the new disulfide bonds further strengthen the covalent interactions within the protein molecules and make the gel structure of the protein stronger, thus improving the BSs binding ability of EWP (Du et al., 2022). The decrease in viscoelasticity of EWPHs occurred after digestion but remained higher than that of the CK group, which could be due to the decrease in the viscoelasticity of D-EWPHs as the structure of the protein shifted from an ordered to a disordered structure in the presence of digestive enzymes, resulting in increased mobility and disruption of the existing network structure (Du et al., 2022). It is also possible that extreme pH disrupts hydrophobic interactions and van der Waals forces. This breaks the disulfide bonds between protein subunits and partially unfolds the tertiary structure of the molecule, making it less viscoelastic.

### 3.11. Peptidomics analysis

In this experiment, qualitative and quantitative peptidomic analysis was performed on the EWP samples before and after enzymatic digestion, and a total of 6071 peptides were identified, and the abundance analysis of the peptides was performed, and the abundance ratio  $\geq 10$  or  $\leq 0.1$  and  $P$  value adjust  $\leq 0.05$  were used as the differential peptide screening conditions, and more significantly differentially expressed peptides were screened, as shown in Table 1(A).

Following the identification of peptides with hypocholesterolemic activity, 67 peptides with similar amino acid sequences were screened from EWPHs, D-CK, and D-EWPHs with significant differences in expression compared to the CK group. As shown in Table 1(B), most of the results were derived from ovalbumin. Most of these peptides had a molecular weight between 300 and 2300 Da. According to Ye et al. (2023), cholesterol-lowering peptides in tea proteins have a molecular weight below 3 kDa. Further, based on the probability prediction of biological activity of the differentially significant peptides by the peptide library (<http://distilldeep.ucd.ie/PeptideRanker/>), the selection was adjusted upward from 0.5 to 0.8, reducing false positives, and peptides with scores  $>0.8$  were identified as potentially biologically active peptides (Mudgil et al., 2022). Comparatively, FVLPM and GGGVW, which contain cholesterol-lowering fragments, have a bioactivity potential of  $>0.8$ . As a consequence, these two peptides may be effective in lowering cholesterol levels.

The relative abundance of EWP can be determined by analyzing the thermogram results of EWP before and after enzymatic digestion, as well as peptide abundance, as depicted in Fig. 4 (A). A darker red color indicates a greater relative abundance of peptides, whereas a lighter blue color indicates a lower relative abundance. A comparison of CK and EWPHs groups revealed that EWP released more peptides after enzymatic digestion, and both groups were subjected to simulated

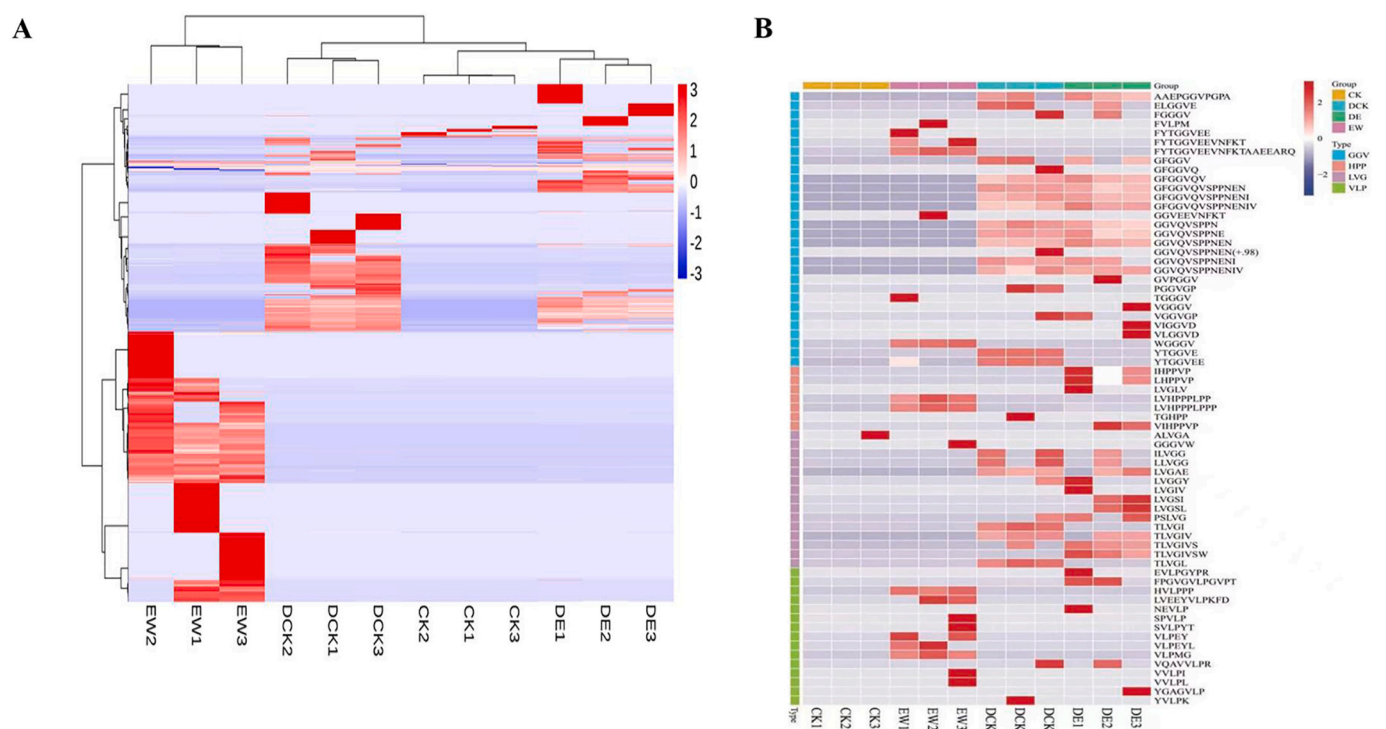


**Fig. 4.** (A) Analysis of EWP heat map before and after enzymatic hydrolysis and digestion. Where EW: EWP; DCK: D-CK; DE: D-EWPHs; where the darker red color represents the higher relative abundance of peptides and the darker blue color represents the lower relative abundance of peptides, and (B) Heat map analysis of EWP cholesterol-lowering peptide before and after enzymolysis and digestion. Where EW: EWP; DCK: D-CK; DE: D-EWPHs; where the darker red color represents the higher relative abundance of peptides and the darker blue color represents the lower relative abundance of peptides. (For interpretation of the references to color in this figure legend, the reader is referred to the web version of this article.)

gastrointestinal stimulation. Due to the action of digestive enzymes and pH, which further degraded the protein and created more small molecule peptide fragments after digestion, the abundance of peptides increased significantly. Further, the changes in thermogram analysis results were associated with the changes in protein structure, which were caused by an increased degree of protein folding and the exposure of more binding sites.

The thermogram analysis performed for the potential hypocholesterolemic peptides of EWP screened in Table 1(B) according to their abundance is shown in Fig. 4 (B). Compared to the CK group, the four groups of cholesterol-lowering fragments showed a significant increase in the abundance of peptides corresponding to EWP, D-CK and D-EWPHs. These peptides with hypocholesterolemic activity may play a role in EWP after enzymatic digestion and digestion, giving EWP a high hypocholesterolemic efficacy, providing the foundation for an in-depth study of the hypocholesterolemic activity of these peptides and provides a basis for future designing and simulation of hypocholesterolemic peptides.

### 3.12. Molecular docking

The schematic diagram in Fig. 5 (A1-A3) depicts the intermolecular forces between ovalbumin and BSs molecules, as predicted by PLIP analysis. It is evident from the figure that hydrophobic interactions and hydrogen bonds are the predominant interactions between OVA and BSs molecules.

As shown in Fig. 5 (B1-B3), the interaction types and docking positions between OVA and three BSs molecules respectively, the binding force between OVA and BSs molecules is mainly hydrogen bonding, and its binding is more stable at low docking energy. SC mainly interacts with GLY-1 (glycine), ASN-54 (asparagine), LYS-61 (lysine), LEU-62 (leucine), etc. in OVA. The lowest molecular docking energy is  $-8.25$ ; STC mainly interacts with GLU-108 (glutamic acid), ARG-110

(arginine), TYR-111 (tyrosine) and other amino acid residues in ovalbumin, and the lowest molecular docking energy is  $-7.16$ ; SDC mainly interacts with GLU-108, ARG-110, TYR-111, GLU-275 and other residues in ovalbumin, and the lowest molecular docking energy is  $-7.16$ . TYR-111 and GLU-275 in ovalbumin, with a minimum molecular docking energy of  $-7.33$ .

Consequently, these hydrophobic amino acids interact with BSs molecules to influence egg white proteins' functional properties (Gao et al., 2018). There may be a reason why BSs binds more strongly to the enzymatically modified EWP and digested CK groups because more hydrophobic residues are exposed. As a result, egg white proteins' ability to bind to BSs molecules may be enhanced through enhanced hydrophobic interactions.

## 4. Conclusions

This study investigated the effect of neutral protease digestion on the BSs-binding capacity of EWP through an *in vitro* simulation of gastrointestinal digestion. The results showed that the BSs-binding capacity of EWP remained strong after digestion, mainly due to the exchange of sulfhydryl groups and disulfide bonds, promoting hydrogen bond formation. Structural analysis revealed that smaller particle sizes and low molecular weights promoted BSs-binding, and a disordered structure enhanced the binding capacity. Additionally, the exposure of tryptophan and tyrosine residues, increased apparent viscosity, viscoelasticity, and surface hydrophobicity, as well as decreased sulfhydryl content, all contributed to enhanced BSs-binding. Although D-EWPHs exhibited a more stable secondary structure after digestion, its BSs-binding capacity decreased slightly. However, compared to CK, the exposure of more hydrophobic groups still resulted in a higher BSs-binding capacity. Peptidomic analysis identified potential cholesterol-lowering active peptides, such as FVLPM and GGGVW. Molecular docking analysis further indicated that the interaction between EWP and

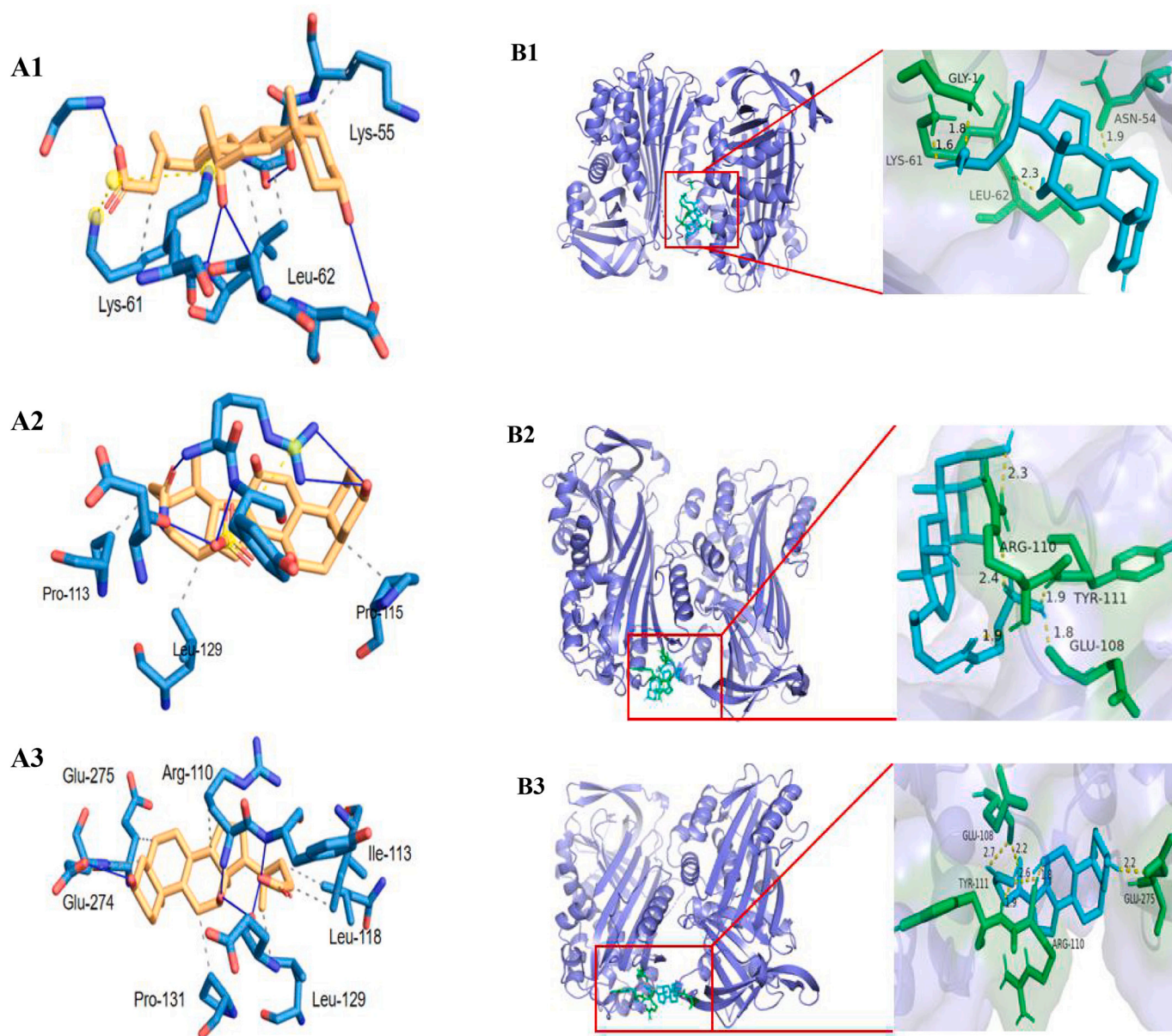


**Fig. 5.** (A1-A3) Prediction of the interaction between ovalbumin and bile salt molecules. Where A1 is the interaction force between ovalbumin and sodium cholate molecules; A2 is the interaction force between ovalbumin and sodium taurocholate molecules; A3 is the interaction force between ovalbumin and sodium deoxycholate molecules; where blue bar structures represent amino acid residues in ovalbumin that interact with bile salt molecules, yellow bar structures are bile salt molecules, gray dashed lines connect hydrophobic interactions, and blue solid lines connect hydrogen bonding interactions. (B1-B2) Three-dimensional molecular docking image of ovalbumin and bile salt. Where B1 is the molecular docking image of ovalbumin with sodium cholate; B2 is the molecular docking image of ovalbumin with sodium taurocholate; B3 is the molecular docking image of ovalbumin with sodium deoxycholate; where the green bar structure represents the amino acid residues in ovalbumin that interact with the bile salt molecule, and the blue bar structure is the bile salt molecule. (For interpretation of the references to color in this figure legend, the reader is referred to the web version of this article.)

BSs primarily involves hydrophobic interactions and hydrogen bonds, and enzyme digestion may expose more hydrophobic amino acid residue sites.

This study explored the relationship between BSs binding capacity and EWPs structure under *in vitro* simulated gastrointestinal digestion conditions, revealing that enzyme digestion significantly affects the binding capacity between EWPs and BSs. Through in-depth research, we clarified the mechanism of structural changes, providing new insights into the structural modification and biological activity enhancement of EWPs. Simultaneously, peptidomic analysis revealed changes in small molecule structures after enzyme digestion and identified potential cholesterol-lowering active peptides. Furthermore, we conducted molecular docking studies to gain a deeper understanding of the interaction

mechanisms between EWPs and BSs. However, this study has not yet involved *in vivo* experiments to validate the effectiveness of *in vitro* results, and the biological function verification of cholesterol-lowering active peptides is still insufficient. Future work will focus on validating these findings and exploring their potential for practical applications.

#### CRediT authorship contribution statement

**Chunjie Liu:** Writing – original draft, Methodology, Formal analysis, Data curation. **Yating Wu:** Investigation, Data curation. **Guoguo Jin:** Writing – review & editing, Data curation. **Baocai Xu:** Conceptualization. **Lin Mei:** Writing – review & editing, Methodology, Funding

**Table 1**

(A) Number of different peptides screened by EWP before and after enzymolysis and digestion, and (B) Potential cholesterol-lowering peptides of EWP before and after enzymatic hydrolysis and digestion.

	Processing group	Processing group	Up	Down
Combination 1	EWPHs	CK	1290	48
Combination 2	D-EWPHs	D-CK	193	467
Combination 3	D-CK	CK	1102	44
Combination 4	D-EWPHs	EWPHs	745	1253

Peptides	Mw	Cholesterol lowering clip
HVLPPP	658.3802	VLP (Chen et al., 2020)
LVEEYVLPKFD	1350.707	
FPGVGVLPGVPT	1138.639	
VLPEYL	732.4058	
VLPMG	515.2778	
VLPEY	619.3217	
SVLPYT	678.3588	
EVLPGYPR	929.497	
NEVLP	570.3013	
VQAVVLP	880.5494	
VVLPL	539.3683	
VVLPI	539.3683	
SPVLP	511.3006	
YGAGVLP	675.3591	
YVLPK	618.3741	
FVLP	605.3247	
FYTGGVEEVNFKTAEEARQ	2245.065	GGV (Ye et al., 2023)
GFGGVQVSPNNENI	1413.689	
GFGGVQVSPNNEN	1300.605	
GFGGVQVSPNNENIV	1512.757	
GGVQVSPNNEN	1096.515	
FYTGGVEEVNFKT	1489.709	
GGVQVSPNNENI	1209.599	
GGVQVSPNNENIV	1308.667	
YTGGVEE	753.3181	
GGVQVSPNNE	982.4719	
GGVEEVNFKT	1078.529	
FYTGGVEE	900.3865	
GGVQVSPN	853.4294	
YTGGVE	624.2755	
WGGGV	474.2227	
GFGGVQV	662.3387	
GGVQVSPNNEN	1097.499	
FGGGV	435.2118	
GFGGV	435.2118	
PGGVGP	482.2489	
TGGGV	389.191	
AAEPGGVPGPA	921.4556	
GVPGGV	484.2645	
GFGGVQ	563.2703	
ELGGVE	602.2911	
VLGGVD	558.3013	
VIGGVD	558.3013	
VGGVGP	484.2645	
VGGGV	387.2118	
GGGVW	474.2227	
TLVGIVSW	873.496	LVG (Ye et al., 2023)
LVGGY	507.2693	
TLVGI	501.3162	
TLVGL	501.3162	
LVGAE	487.2642	
TLVGIV	600.3846	
ILVGG	457.29	
LLVGG	457.29	
LVGSI	487.3006	
LVGSL	487.3006	
TLVGIVS	687.4167	
PSLVG	471.2693	
ALVGA	429.2587	

**Table 1 (continued)**

Peptides	Mw	Cholesterol lowering clip
LVGIV	499.337	
LVGLV	499.337	
LVHPPPLPPP	1062.623	HPP (Banno et al., 2019)
LVHPPPLPP	965.5698	
VIHPPVP	757.4486	
IHPPVP	658.3802	
LHPPVP	658.3802	
TGHPP	507.2441	

acquisition, Conceptualization.

### Declaration of competing interest

We have made substantial contributions to the design of the work and made the analysis and interpretation of data for the work.

We have revised it critically for important intellectual content and have approved the final version to be published.

We agree to be accountable for all aspects of the work in ensuring that questions related to the accuracy and integrity of any part of the work are appropriately investigated and resolved.

All authors have read the final version and approved it for submission to your CEO. There is no conflict of interest.

All authors who have made substantial contributions to the work reported in the manuscript.

### Data availability

Data will be made available on request.

### Acknowledgement

#### Role of the funding source.

#### Funding

This study was supported by the 2021 Anhui Major Science and Technology Special Project [grant no. d06050001] and Anhui Provincial Department of Education collaborative innovation project [grant no. GXXT-2023-051].

### References

- Abeyrathne, E. D. N. S., Huang, X., & Ahn, D. U. (2018). Antioxidant, angiotensin-converting enzyme inhibitory activity and other functional properties of egg white proteins and their derived peptides – A review. *Poultry Science*, 97(4). <https://doi.org/10.3382/ps/pex399>
- Ai, M., Xiao, N., & Jiang, A. (2020). Molecular structural modification of duck egg white protein conjugates with monosaccharides for improving emulsifying capacity. *Food Hydrocolloids*, 111. <https://doi.org/10.1016/j.foodhyd.2020.106271>
- Alberto, R. B. A. K., Ignasi, S. G. H. P. A. C.-G. J., Sofia, M. J. P. J., Jaume, P.-S., & Enric, G. (2023). Bile salt dietary supplementation promotes growth and reduces body adiposity in gilthead seabream (*Sparus aurata*). *Aquaculture*, 566, Article 739203. <https://doi.org/10.1016/j.aquaculture.2022.739203>
- Ashraf, J., Liu, L., Awais, M., Xiao, T., & Zhou, S. (2020). Effect of thermosonication pre-treatment on mung bean and white kidney bean proteins: Enzymatic hydrolysis, cholesterol lowering activity and structural characterization. *Ultrasonics Sonochemistry*, 66, Article 105121. <https://doi.org/10.1016/j.ultsonch.2020.105121>
- Banno, A., Wang, J., Okada, K., Mori, R., Mijiti, M., & Nagaoka, S. (2019). Identification of a novel cholesterol-lowering dipeptide, phenylalanine-proline (FP), and its down-regulation of intestinal ABCA1 in hypercholesterolemic rats and Caco-2 cells. *Scientific Reports*, 9(1), 19416. <https://doi.org/10.1038/s41598-019-56031-8>
- Barbana, C., Boucher, A. C., & Boye, J. I. (2011). In vitro binding of bile salts by lentil flours, lentil protein concentrates and lentil protein hydrolysates. *Food Research International*, 44(1), 174–180. <https://doi.org/10.1016/j.foodres.2010.10.045>
- Bellesi, F. A., & Pilosof, A. M. R. (2021). Potential implications of food proteins-bile salts interactions. *Food Hydrocolloids*, 118(1), Article 106766. <https://doi.org/10.1016/j.foodhyd.2021.106766>
- Besseling, H., Huijgen, G. K., Kastelein, J. J. P. H., & A. B. (2016). Statins in familial hypercholesterolemia: Consequences for coronary artery disease and all-cause mortality. *Journal of the American College of Cardiology*, 68(68–14). [https://doi.org/10.1161/circ.132.suppl\\_3.18995](https://doi.org/10.1161/circ.132.suppl_3.18995)

- Celus, I., Brijs, K., & Delcour, J. A. (2007). Enzymatic hydrolysis of brewers' spent grain proteins and technofunctional properties of the resulting hydrolysates. *Journal of Agricultural & Food Chemistry*, 55(21), 8703. <https://doi.org/10.1021/jf071793c>
- Chen, G., Chen, Y., Hou, Y., Huo, Y., Gao, A., Li, S., & Chen, Y. (2020). Preparation, characterization and the in vitro bile salts binding capacity of celery seed protein hydrolysates via the fermentation using *B. Subtilis*. *LWT-food. Science & Technology*, 117, Article 108571. <https://doi.org/10.1016/j.lwt.2019.108571>
- Colosimo, R., Mulet-Cabero, A. I., Warren, F. J., Edwards, C. H., & Wilde, P. J. (2020). Mycoprotein ingredient structure reduces lipolysis and binds bile salts during simulated gastrointestinal digestion. *Food & Function*, 11(12). <https://doi.org/10.1039/d0fo02002h>
- Du, J., Zhou, C., Xia, Q., Wang, Y., Geng, F., He, J., Sun, Y., Pan, D., & Cao, J. (2022). The effect of fibrin on rheological behavior, gelling properties and microstructure of myofibrillar proteins. *LWT-Food Science & Technology*, 153, Article 112457. <https://doi.org/10.1016/j.lwt.2021.112457>
- Gao, A., Dong, S., Chen, Y., Chen, G., Li, S., & Chen, Y. (2018). In vitro evaluation and physicochemical characteristics of casein phosphopeptides-soluble dietary fibers copolymers as a novel calcium delivery system. *Food Hydrocolloids*, 79, 482–490. <https://doi.org/10.1016/j.foodhyd.2018.01.024>
- Gu, X., Campbell, L. J., & Euston, S. R. (2009). Influence of sugars on the characteristics of glucono- $\delta$ -lactone-induced soy protein isolate gels. *Food Hydrocolloids*, 23(2), 314–326. <https://doi.org/10.1016/j.foodhyd.2008.01.005>
- Hu, H., Li-Chan, E. C. Y., Wan, L., Tian, M., & Pan, S. (2013). The effect of high intensity ultrasonic pre-treatment on the properties of soybean protein isolate gel induced by calcium sulfate. *Food Hydrocolloids*, 32(2), 303–311. <https://doi.org/10.1016/j.foodhyd.2013.01.016>
- Huang, L., Ding, X., Dai, C., & Ma, H. (2017). Changes in the structure and dissociation of soybean protein isolate induced by ultrasound-assisted acid pretreatment. *Food Chemistry*, 232, 727–732. <https://doi.org/10.1016/j.foodchem.2017.04.077>
- Karaman, S., Yilmaz, M. T., Dogan, M., Yetim, H., & Kayacier, A. (2011). Dynamic oscillatory shear properties of O/W model system meat emulsions: Linear viscoelastic analysis for effect of temperature and oil concentration on protein network formation. *Journal of Food Engineering*, 107(2), 241–252. <https://doi.org/10.1016/j.jfoodeng.2011.06.016>
- Kashima, Y., Kanematsu, S., Asai, S., Kusada, M., Watanabe, S., Kawashima, T., Nakamura, T., Shimada, M., Goto, T., & Nagaoka, S. (2014). Identification of a novel hypocholesterolemic protein, major Royal Jelly Protein 1. *Derived from Royal Jelly. PLoS ONE*, 9(8), 3. <https://doi.org/10.1371/journal.pone.0105073>
- Klost, M., Giménez-Ribes, G., & Drusch, S. (2020). Enzymatic hydrolysis of pea protein: Interactions and protein fractions involved in fermentation induced gels and their influence on rheological properties. *Food Hydrocolloids*, 105, Article 105793. <https://doi.org/10.1016/j.foodhyd.2020.105793>
- Li, S., Yang, X., Zhang, Y., Ma, H., & Mahunu, G. K. (2016). Effects of ultrasound and ultrasound assisted alkaline pretreatments on the enzymolysis and structural characteristics of rice protein. *Ultrasonics Sonochemistry*, 31, 20–28. <https://doi.org/10.1016/j.ulsonch.2015.11.019>
- Li, T., Hu, J., Tian, R., Wang, K., Li, J., Qayum, A., ... Hou, J. (2021). Citric acid promotes disulfide bond formation of whey protein isolate in non-acidic aqueous system. *Food Chemistry*, 338. <https://doi.org/10.1016/j.foodchem.2020.127819>
- Liu, F., & Tang, C. H. (2014). Emulsifying properties of soy protein nanoparticles: Influence of the protein concentration and/or emulsification process. *Journal of Agricultural & Food Chemistry*, 62(12), 2644. <https://doi.org/10.1021/jf405348k>
- Liu, P., Xu, H., Zhao, Y., & Yang, Y. (2017). Rheological properties of soy protein isolate solution for fibers and films. *Food Hydrocolloids*, 64, 149–156. <https://doi.org/10.1016/j.foodhyd.2016.11.001>
- Liu, Y., Huang, Y., Deng, X., Li, Z., Lian, W., Zhang, G., Zhu, Y., & Zhu, X. (2022). Effect of enzymatic hydrolysis followed after extrusion pretreatment on the structure and emulsibility of soybean protein. *Process Biochemistry*, 116, 173–184. <https://doi.org/10.1016/j.procbio.2022.03.012>
- Malhotra, A., & Coupland, J. N. (2004). The effect of surfactants on the solubility, zeta potential, and viscosity of soy protein isolates. *Food Hydrocolloids*, 18(1), 101–108. [https://doi.org/10.1016/s0268-005x\(03\)00047-x](https://doi.org/10.1016/s0268-005x(03)00047-x)
- Milkiewicz, P., Roma, M. G., Elias, E., & Coleman, R. (2002). Hepatoprotection with tauroursodeoxycholate and  $\beta$  muricholate against tauroolithocholate induced cholestasis: Involvement of signal transduction pathways. *Gut*, 51(1), 113. <https://doi.org/10.1136/gut.51.1.113>
- Mudgil, P., Baba, W., Kamal, H., Fitzgerald, R., Hassan, H., Ayoub, M., Gan, C., & Maqsood, S. (2022). A comparative investigation into novel cholesterol esterase and pancreatic lipase inhibitory peptides from cow and camel casein hydrolysates generated upon enzymatic hydrolysis and in-vitro digestion. *Food Chemistry*, 367, Article 130661. <https://doi.org/10.1016/j.foodchem.2021.130661>
- Nandy, A., Chakraborty, S., Nandi, S., Bhattacharyya, K., & Mukherjee, S. (2019). Structure, activity and dynamics of human serum albumin in a crowded Pluronic F127 hydrogel. *Journal of Physical Chemistry B*. <https://doi.org/10.1021/acs.jpcc.9b00219>
- Pessato, T. B., De Carvalho, N. C., Tavano, O. L., Fernandes, L. G. R., Zollner, R. D. L., & Netto, F. M. (2016). Whey protein isolate hydrolysates obtained with free and immobilized Alcalase: Characterization and detection of residual allergens. *Food Research International*, 83, 112–120. <https://doi.org/10.1016/j.foodres.2016.02.015>
- Pi, X., Fu, G., Dong, B., Yang, Y., Wan, Y., & Xie, M. (2021). Effects of fermentation with *Bacillus natto* on the allergenicity of peanut. *LWT-Food Science & Technology*, 141(1), Article 110862. <https://doi.org/10.1016/j.lwt.2021.110862>
- Shen, X., Fang, T., Gao, F., & Guo, M. (2017). Effects of ultrasound treatment on physicochemical and emulsifying properties of whey proteins pre- and post-thermal aggregation. *Food Hydrocolloids*, 63, 9. <https://doi.org/10.1016/j.foodhyd.2016.10.003>
- Viseu, M. I., Carvalho, T. I., & Costa, S. M. B. (2004). Conformational transitions in  $\beta$ -Lactoglobulin induced by cationic Amphiphiles: Equilibrium studies. *Biophysical Journal*, 86(4), 2392–2402. [https://doi.org/10.1016/s0006-3495\(04\)74296-4](https://doi.org/10.1016/s0006-3495(04)74296-4)
- Wang, T., Chang, C., Cheng, W., Gu, L., Su, Y., Yang, Y., & Li, J. (2023). Combined effect of heating and enzymatic hydrolysis on the dispersibility and structure properties of egg white powder. *Journal of Food Engineering*, 351, Article 111503. <https://doi.org/10.1016/j.jfoodeng.2023.111503>
- Wang, Z., Yang, L., Xue, S., Wang, S., Zhu, L., Ma, T., Liu, H., & Li, R. (2022). Molecular docking and dynamic insights on the adsorption effects of soy hull polysaccharides on bile acids. *International Journal of Food Science & Technology*, 57(6), 3702–3712. <https://doi.org/10.1111/ijfs.15695>
- Xie, H., Zhang, L., Chen, Q., Hu, J., Zhang, P., Xiong, H., & Zhao, Q. (2023). Combined effects of drying methods and limited enzymatic hydrolysis on the physicochemical and antioxidant properties of rice protein hydrolysates. *Food Bioscience*, 52, Article 102427. <https://doi.org/10.1016/j.fbio.2023.102427>
- Xu, Y., Xia, W., & Jiang, Q. (2012). Aggregation and structural changes of silver carp actomyosin as affected by mild acidification with d-gluconic acid  $\delta$ -lactone. *Food Chemistry*, 134(2), 1005–1010. <https://doi.org/10.1016/j.foodchem.2012.02.216>
- Yang, M., Liu, J., Yang, X., Li, S., Li, C., Liu, B., Ma, S., Liu, X., Du, Z., & Zhang, T. (2021). Effect of glycation degree on the in vitro simulated gastrointestinal digestion: A promising formulation for egg white gel with controlled digestibility. *Food Chemistry*, 349, Article 129096. <https://doi.org/10.1016/j.foodchem.2021.129096>
- Ye, H., Xu, Y., Sun, Y., Liu, B., Chen, B., Liu, G., Cao, Y., & Miao, J. (2023). Purification, identification and hypolipidemic activities of three novel hypolipidemic peptides from tea protein. *Food Research International*, 165, Article 112450. <https://doi.org/10.1016/j.foodres.2022.112450>
- Yoshie-Stark, Y., & Waesche, A. (2004). In vitro binding of bile acids by lupin protein isolates and their hydrolysates. *Food Chemistry*, 88(2), 179–184. <https://doi.org/10.1016/j.foodchem.2004.01.033>